UDK 62-136:629.3.015.5
Original scientific article/Izvirni znanstveni članek

ISSN 1580-2949
MTAEC9, 58(3)397(2024)

EXPERIMENTAL INVESTIGATION OF THE VIBRATION-REDUCTION CHARACTERISTICS OF THE SHAFT COATING FOR A TURBOCHARGER

EKSPERIMENTALNA RAZISKAVA KARAKTERISTIK ZMANJŠANJA VIBRACIJ NA TURBOPOLNILNIKU Z OPLAŠČENO GREDJO

Murat Ok[1], Hamit Saruhan[2]

[1]Düzce University, Gümüşova Vocational School, Mechanical and Metal Technologies Department, Düzce, Türkiye
[2]Düzce University, Mechanical Engineering Department, Faculty of Engineering, Düzce, Türkiye

Prejem rokopisa – received: 2024-03-07; sprejem za objavo – accepted for publication: 2024-04-18

doi:10.17222/mit.2024.1128

A turbocharger is a system that is fitted to automotive engines to increase performance and efficiency by taking air at atmospheric pressure, compressing it to a higher pressure and passing the compressed air into the engine via the inlet valves. A turbocharger consists of a turbine and a compressor impeller interconnected with a shaft supported in most cases by journal bearings. The shaft is one of most crucial components of a turbocharger system and it operates at high speed. The shaft vibrations are an inherent phenomenon and they are travelling to the surrounding structure, effecting the stability and reliability of the turbocharger system. The selection of the appropriate shaft-material property is a critical parameter among the parameters that affect the vibration of the system. This study focuses on exploring whether it is possible to reduce the shaft vibration using different types of coating materials, including aluminum chromium nitride (AlCrN), titanium nitride (TiN) and aluminum titanium nitride (AlTiN), each having thicknesses of (2, 4, and 6) µm, for a shaft made of AISI 4140 alloy steel. The inherent natural vibration properties, such as the resonant frequencies, damping, and mode shapes of the turbocharger shaft with and without coating, were obtained by conducting an experimental modal analysis through measurements of the frequency-response function, which is about curve fitting the data using a predefined mathematical model of the turbocharger shaft. The results were validated numerically with the finite element method. From overall results, it was observed that the AlCrN, TiN, and AlTiN coating thicknesses have a small effect on the resonant frequencies, but a good damping effect. The resonant response of the turbocharger shaft at resonant frequencies was suppressed remarkably by the AlCrN and AlTiN coatings, especially those having a thickness of 6 and 4 µm.

Keywords: turbocharger shaft, shaft coating, vibration damping coating, modal analysis

Turbinski polnilnik je naprava oziroma sistem, ki je vgrajen v določene avtomobilske motorje z namenom izboljšanja njihovih lastnosti in učinkovitosti. Naprava nasesava zrak iz okolice pri normalnem zračnem tlaku, ga skomprimira na višji tlak in vodi v motor z notranjim izgorevanjem preko vstopnih ventilov. Turbinski polnilnik je sestavljen iz turbine in kompresorskega pogonskega kolesa, ki sta med seboj povezana z uležajeno gredjo. Gred je ena od najpomembnejših komponent turbinskega polnilniškega sistema, ki obratuje pri zelo visokih hitrostih. Vibracije gredi so naravni inherentni pojav, ki vpliva tudi na vse ostale dele sistema in s tem vpliva tudi na njegovo stabilnost in zanesljivost. Izbira primernega materiala gredi je kritični parameter med parametri, ki vplivajo na vibracije sistema. V tem članku avtorja opisujeta študijo s pomočjo katere sta skušala ugotoviti, ali se lahko zmanjšajo vibracije gredi z uporabo primernega materiala za njeno oplaščenje. Za oplaščenje so izbralialuminij-krom nitrid(AlCrN), titan nitrid (TiN) in aluminij-titan nitrid(AlTiN). Izbrane debeline plasti, nanešene na legirano jeklo vrste AISI4140 so bile (2, 4 in 6) µm. Lastnosti inherentnih naravnih vibracij kot so resonančna frekvenca, dušenje in oblika gredi turbinskega polnilnika z in brez prevleke so bile dobljene s pomočjo eksperimentalne modalne analize preko merjenja funkcije frekvenčnega odgovora. Za prilagoditev funkcijske odvisnosti sta avtorja uporabila pred-definiran matematični model gredi turbinskega polnilnika. Rezultate sta ovrednotila numerično z metodo končnih elementov. Iz dobljenih rezultatov sta avtorja ugotovila, da ima debelina AlCrN, TiN in AlTiN prevlek majhen vpliv na resonančne frekvence toda imajo velik vpliv na učinek dušenja. Resonančni odgovor gredi turbinskega polnilnika je bil opazno zadušen pri prevlekah iz AlCrN in AlTiN, še posebej pri debelinah 6 mm in 4 mm.

Ključne besede: gred turbinskega polnilnika, vrste prevlek gredi, dušenje vibracij, modalna analiza

1 INTRODUCTION

Turbocharger systems started as a means to increase the power output of an engine.[1] They are now more prevalent in the automotive industry and are fitted to engines in response to fuel-efficiency requirements around the world. A turbocharger is a system that is fitted to internal combustion engines to improve the overall efficiency and performance by increasing the power output while lowering the fuel consumption. A turbocharger consists of a turbine and a compressor impeller interconnected with a shaft supported in most cases by journal bearings.[2] It is similar to a pump that pushes more air into the air-fuel mixture of the engine's cylinders. More air means more oxygen and more efficient gasoline combustion, helping the engine to produce more power.[3] The turbocharger operates at high rotational speeds of up to 300,000 min^{-1}. There are several literature reviews that the reader can refer to for more detailed background information about turbochargers.[4–8] There is a particularly high level of in-

*Corresponding author's e-mail:
muratok@duzce.edu.tr (Murat Ok)

terest in reducing the amplitude of vibration of the turbocharger. Many studies have been carried out on different sources of vibrations that are related to turbocharger performance.[9–14] The research to date has tended to focus on turbine, compressor impeller and bearing vibration's influence on the performance of the turbocharger system rather than the turbocharger shaft's influence.[15–18] The turbocharger shaft is the most important component in the turbocharger and the vibration of the turbocharger shaft greatly affects the performance of the engine. The inherent damping of the turbocharger shaft's materials is often low, to add coating can provide significant reductions to the amplitude values of the vibration, enabling more efficient performance of the turbocharger system. The influence of coating on the vibration characteristics of the turbocharger shaft are not well researched. Therefore, this study tries to figure out the influence of the type and thickness of the coating employed on the turbocharger's shaft for vibration reduction in the turbocharger system. In this study, three different types of coating materials including aluminum chromium nitride (AlCrN), titanium nitride (TiN) and aluminum titanium nitride (AlTiN), each having thicknesses of 2, 4, and 6 µm (microns), were applied to the turbocharger shaft's surface. An experimental modal analysis (EMA) was used to measure the inherent dynamic characteristic, called the resonant (natural) frequencies, damping, and mode shapes, of the turbocharger shaft. Also, resonant frequencies are determined and validated numerically using the finite-element method (FEM).

EMA is one of the methods used to determine the inherent natural vibration properties of a structure in the forms of resonant frequencies, damping factors, and mode shapes.[19] Resonant frequencies are the frequencies at which the structure resonates. The mass, stiffness, and damping properties of the material and the boundary conditions of the structure are used to determine the modes to characterize the resonant vibration.[20] Thus, the mode shapes represent specific deflection patterns associated with the resonant frequencies, which are dependent on the way the mass and stiffness are distributed within the structure.[21] The relationship between the applied force (input) and the vibration response (output) of the turbocharger shaft is determined using the frequency-response function (FRF), which is an extension of the EMA.

2 EXPERIMENTAL SET-UP

Specimens for the experiments were prepared from an AISI 4140 alloy steel shaft material composed of chromium, carbon, manganese, molybdenum, phosphorus, silicon, and sulfur. The AISI 4140 alloy steel has distinct mechanical characteristics that make it valuable for a turbocharger shaft due to the good toughness, impact resistance, and fatigue strength.

For the experiments, a total of ten specimens were prepared and categorized as four sets given in **Figure 1** and **Table 1**. Besides one uncoated shaft, three shafts were separately subjected to coating materials as follows: AlCrN, TiN and AlTiN each having thickness of 2, 4, and 6 µm. AlCrN, TiN and AlTiN coatings were applied to the turbocharger shaft surface by an industrial cathodic arc physical vapor deposition (PVD) process, which involves vaporizing a small amount of titanium and nitrogen in a vacuum chamber and deposition of the vapor onto the surface. The process is selected since it finds wide range applications in various industries due to its ability to deposit a uniform thin film. A coating process unit (brand: PLATIT model: PL1011) was used.

Table 1: Specification of Test Specimens

Specimens	Coating	Coating Materials			Coating Thickness, µm		
		AlCrN	TiN	AlTiN	2	4	6
Uncoated							
AlCrN-2	x	x			x		
TiN-2	x		x		x		
AlTiN-2	x			x	x		
AlCrN-4	x	x				x	
TiN-4	x		x			x	
AlTiN-4	x			x		x	
AlCrN-6	x	x					x
TiN-6	x		x				x
AlTiN-6	x			x			x

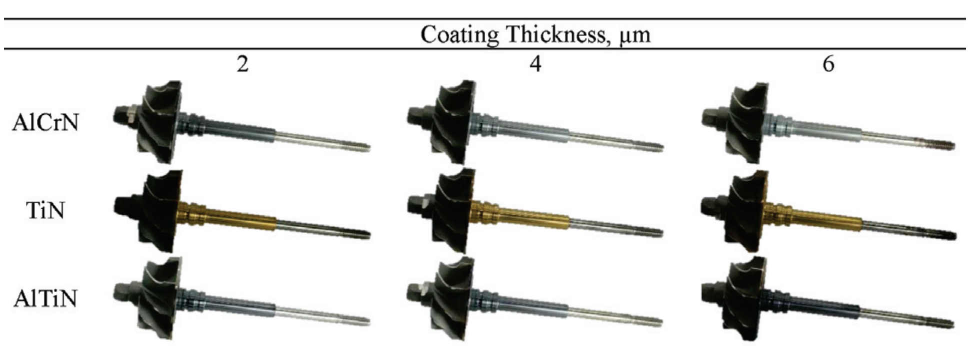

Figure 1: Test Specimens

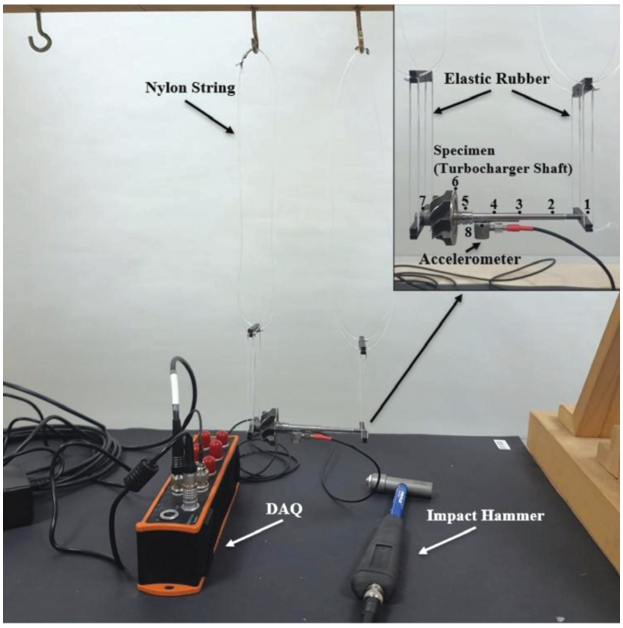

Figure 2: Test rig

AlCrN: aluminum chromium nitride TiN: titanium nitride AlTiN: aluminum titanium nitride

In order to investigate the effect of the coating applied to the turbocharger shaft's surface for vibration reduction in turbocharger system using the EMA, a large number of tests were conducted on the test rig shown in **Figure 2**. Each specimen is suspended by rubber bands attached to nylon strings to simulate the free-free boundary conditions. A series of initial trials were conducted to get the proper position of the excitation points. Seven hammer-strike location points were selected on the turbocharger shaft and the turbine impeller. The turbocharger shaft was excited using Dytran-type force transducers, i.e., an impact hammer (Model: 5800B3T, Sensitivity: 11.24 mV/N) at all the predefined location points. A steel type (model: 6250A) of impact hammer tip was used to ensure a quality measurement. The response was measured using one uniaxial accelerometer (MMF Type, Model: KS78C.100, sensitivity: 100 mV/g) having a frequency response from 0.2 Hz to 20 kHz attached to the turbocharger shaft with glue at location point 8. A multi-channel data-acquisition (DAQ) device KRYPTON-8xACC having a sampling rate up to 20 kHz per channel was used to acquire the data. The modal parameters – resonant frequencies, damping factors, and mode shapes – are extracted from the generated FRFs using Dewesoft hardware and software.

3 RESULTS AND DISCUSSION

The inherent natural vibration properties such as the resonant frequencies, damping, and mode shapes of the turbine impeller shaft of the turbocharger with AlCrN, TiN, and AlTiN coatings each having thickness of (2, 4, and 6) μm were obtained using the EMA, and for validation of results, the FEM was implemented. Four turbine impeller shaft sets were tested. These were a set of uncoated turbine impeller shaft (Uncoated), a set of the turbine impeller shafts with AlCrN, TiN, and AlTiN coatings each having thickness of 2 μm (AlCrN-2, TiN-2, and AlTiN-2), a set of the turbine impeller shafts with AlCrN, TiN, and AlTiN coatings each having thickness of 4 μm (AlCrN-4, TiN-4, and AlTiN-4), a set of the turbine impeller shafts with AlCrN, TiN, and AlTiN coatings each having thickness of 6 μm (AlCrN-6, TiN-6, and AlTiN-6). **Table 2** shows the first two resonant frequencies of the bending modes of the specimens (Uncoated, AlCrN-2, TiN-2, AlTiN-2, AlCrN-4, TiN-4, AlTiN-4, AlCrN-6, TiN-6, AlTiN-6) measured from the EMA and predicted numerically from the FEM for the validation of the results. Since the sampling frequency of the data-acquisition device is limited, the first two resonant frequencies were obtained.

In general, the experimental measurement of the resonant frequencies is in good agreement with the results from the FEM. The resonant frequency from the EMA is generally lower than those obtained using the FEM. This is because the impact hammer's mass contributions to the overall specimen mass. However, it should be noted that the resonant frequencies obtained from the EMA are higher than those obtained using the FEM, except for the specimen (TiN-6) at Mode 2. This means that the specimens have greater stiffness or smaller mass than the FEM model due to either an imprecise manufacturing or coating process.

Table 2: Resonant frequencies from the EMA and the FEM

Specimens	Coating Thickness, μm	Resonant Frequencies, Hz			
		Mode 1		Mode 2	
		EMA	FEM	EMA	FEM
Uncoated	0	1610.7	1572.2	4844.2	4532.0
AlCrN-2	2	1620.6	1584.4	4735.7	4573.9
TiN-2		1634.0	1604.0	4793.4	4673.4
AlTiN-2		1633.3	1599.4	4783.6	4659.0
AlCrN-4	4	1634.9	1603.1	4847.9	4665.9
TiN-4		1647.8	1620.3	4873.6	4721.3
AlTiN-4		1675.9	1611.7	4914.2	4693.8
AlCrN-6	6	1642.3	1611.2	4815.6	4691.4
TiN-6		1674.9	1635.4	4624.1	4771.0
AlTiN-6		1711.3	1623.5	4729.0	4731.7

The results obtained from the EMA for the first two resonant frequencies of the bending modes of the specimens are given in **Figure 3.** It can be seen from the results that the resonant frequencies of the specimens increase with an increase of the coating thickness at Mode 1. However, the resonant frequencies of the specimens with a coating thickness of 4 μm were much higher than the coating thicknesses of (2 and 6) μm at Mode 2.

Each characteristic displacement pattern called a mode shape corresponds to a resonant frequency. The degree of participation of each mode in the overall vibra-

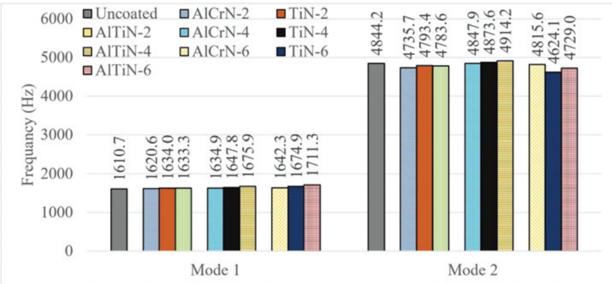

Figure 3: Resonant frequencies from the EMA

tion is determined from a model of the specimen to animate the mode shapes at each of the measured resonant frequencies. Although continuous systems have an infinite number of mode shapes, it is sufficient to use a number of modes to describe the detailed covering of the dynamic behavior of the specimens. Due to the sample-rate limitations of the data-acquisition device used, the first two mode shapes were determined and presented in **Figure 4**. The data was obtained using the frequency range up to 7812.5 Hz and a frequency resolution of 1 Hz. It can be seen in **Figure 4** that the complete dynamic behavior of all the specimens is viewed as a set of individual modes of vibration, each having a characteristic resonant frequency, damping, and mode shape.

The FRF plots of all the specimens are determined as output results by impacting the specimens using the force hammer. The FRF presents the ratio of the vibration response and the applied force of the specimens over the frequency range. The comparative FRF plots for all the specimens are given in **Figure 5**. The plots corresponding to the resonant frequencies of the specimens are presented in terms of acceleration/force versus frequency. There is a much more reduced vibration amplitude at Mode 2 compared with Mode 1. It can be observed that the response plots determined for specimens AlCrN-6 and AlTiN-4 show more accumulation of vibration energy with adequate dissipation. They have a wider modal peak, which indicates a higher damped mode. The overall amplitude of the FRF is higher when comparing the specimens TiN-2, TiN-4, TiN-6 to AlCrN-2, AlCrN-4, AlCrN-6, AlTiN-2, AlTiN-4, AlTiN-6 at Mode 1. In comparison with the overall specimens at Mode 1 and Mode 2, the damping ratio of the specimens (AlCrN-6 and AlTiN-4) sharply increased and also, the overall vibration amplitude peak attenuation value was reached at about 11.2 dB (with reference 1 m/s^2/N) in the 600–2200 Hz frequency band at Mode 1 and 7.5 dB (with reference 1 m/s2/N) in the 4000–5200 Hz frequency band at Mode 2. Thus, a higher damping ratio indicated absorbing the energy and reducing the amplitude of the vibration at resonant frequencies at Mode 1 and Mode 2. The AlCrN-6 and AlTiN-4 specimens have an obvious vibration-suppression effect on the turbocharger shaft.

Coherence was used to assess the validation and quality of the FRF measurement. Coherence, which varies from zero to one is used to ensure a correlation between the vibration response and the applied force excitation that is how well they are related to each other. When the coherence is equal to one, the applied force excitation and vibration response are completely related. It can be seen from the coherence plots in **Figure 5** that the coherence overall is close to one across the frequency range. However, it is known that coherence is low at anti-resonance.

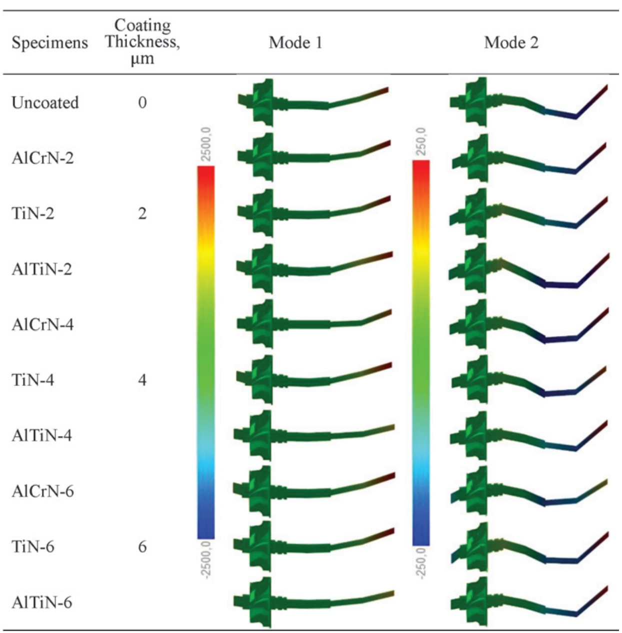

Figure 4: Mode shapes from the EMA

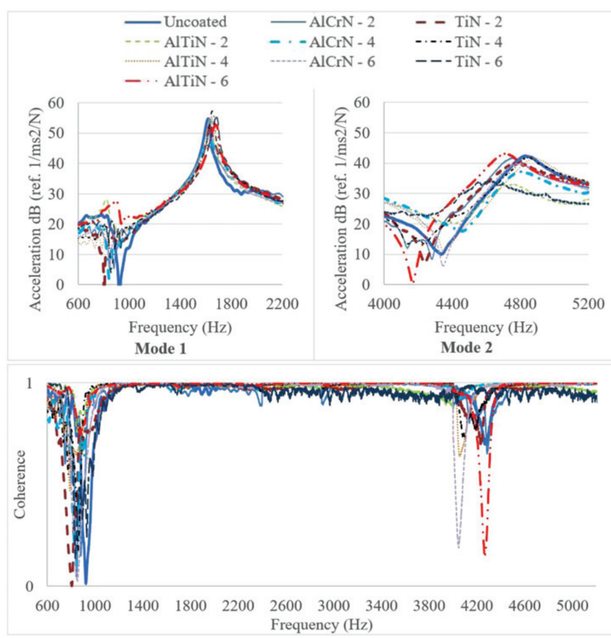

Figure 5: The FRF and coherence plot for specimens

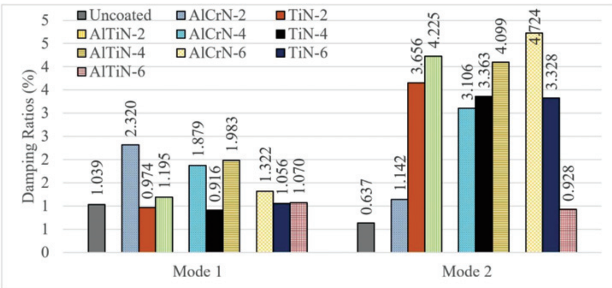

Figure 6: Damping ratios from the EMA

The damping ratios associated with each mode of the specimens are determined from the sharpness of the resonant peaks by half power bandwidth (approximately 3 dB down from the resonant peaks) calculation are presented in **Table 3** and **Figure 6**. It can be seen from **Figure 6** that there are much more increased damping ratios in the corresponding resonant response results at Mode 2 of the specimens compared with the response results at Mode 1 of the specimens, except the uncoated, AlCrN-2 and AlTiN-6 specimens. Also, it can be noted that even the thinner coatings (AlCrN-2, TiN-2, AlTiN-2) also achieved better damping performance than the uncoated specimen at Mode 2 and mostly at Mode 1.

Table 3: Damping ratios from the EMA

Specimens	Coating Thickness, μm	Damping Ratios, %	
		Mode 1	Mode 2
Uncoated	0	1.039	0.637
AlCrN-2	2	2.320	1.142
TiN-2		0.974	3.656
AlTiN-2		1.195	4.225
AlCrN-4	4	1.879	3.106
TiN-4		0.916	3.363
AlTiN-4		1.983	4.099
AlCrN-6	6	1.322	4.724
TiN-6		1.056	3.328
AlTiN-6		1.070	0.928

The resonant response of the turbocharger shaft at resonant frequencies is suppressed remarkably by the AlCrN-6 and AlTiN-4 coatings compared to the AlCrN-2, TiN-2, AlTiN-2, AlCrN-4, TiN-4, TiN-6, AlTiN-6 coatings. From the overall results, it can be noted that the AlCrN, TiN, AlTiN coating thicknesses have a small effect on the resonance frequencies, but a good damping effect. Thus, the damping performance of the specimens was considerably improved by the AlCrN, TiN, AlTiN coatings, especially by the AlCrN-6 and AlTiN-4 coatings compared to the AlCrN-2, TiN-2, AlTiN-2, AlCrN-4, TiN-4, TiN-6, AlTiN-6 coatings.

4 CONCLUSIONS

The EMA is conducted to obtain the effect of different types and thicknesses of coating on the dynamic characteristics in terms of modal parameters called resonant frequencies, damping ratios, and mode shapes of a turbocharger shaft. The results showed that the coatings (AlCrN, TiN, AlTiN) have a small effect on the resonant frequencies, but a good effect on damping performance of the turbocharger shaft. The resonant response amplitude of the turbocharger shaft at resonant frequencies is suppressed remarkably by AlCrN-6 and AlTiN-4 coatings compared to the AlCrN-2, TiN-2, AlTiN-2, AlCrN-4, TiN-4, TiN-6, AlTiN-6 coatings. It can be concluded that the coating can improve the dynamic characteristics, especially the vibration-damping performance of the turbocharger shaft by adjusting the coating thickness. So that to improve the damping capacity of the turbocharger shaft, it is essential that the properties of the coating should be known and efficient coating type and proper coating thickness implementation should be taken with care. Thus, the damping-capacity variation can be implemented efficiently by adjusting the coating type and thickness.

On the basis of the promising findings presented in this study, a possible future study using a compressor impeller interconnected with the turbocharger shaft specimens supported by journal bearings at different operating speeds for investigating vibration damping performance of a turbocharger system could be conducted.

Acknowledgment

This study is financial supported by the Scientific Research Project (BAP) Coordination Unit of Düzce University (Project No: 2022.06.05.1308).

5 REFERENCES

[1] S. Dasgupta, P. Sarmah, P. P. Borthakur, Application of variable geometry turbine turbochargers to gasoline engines – A review, IOP Conf. Ser. Mater. Sci. Eng., 943 (**2020**) 1 012010, doi:10.1088/1757-899X/943/1/012010

[2] P. Sass, Literature Research on Experimental Investigations of Automotive Turbocharger Rotordynamics, Acta Tech. Jaurinensis, 12 (**2019**) 4, 268–293, doi:10.14513/actatechjaur.v12.n4.498

[3] B. Sumali, A. Gunawan, A. A. Maharano, The effect of flushing and surging air treatment on the turbocharger on high exhaust gas temperature on mv ship. Beautiful food, Dinasti Int. J. Digit. Bus. Manag., 3 (**2022**) 6, 1013–1025, doi:10.31933/DIJDBM.V3I6.1517

[4] M. Muqeem, M. Ahmad, A. F. Sherwani, Turbocharging of Diesel Engine for Improving Performance and Exhaust Emissions: A Review, IOSR J. Mech. Civ. Eng. Ver. III, 12 (**2015**) 4, 2278–1684, doi:10.9790/1684-12432229

[5] A. J. Feneley, A. Pesiridis, A. M. Andwari, Variable Geometry Turbocharger Technologies for Exhaust Energy Recovery and Boosting – A Review, Renew. Sustain. Energy Rev., 71 (**2017**), 959–975, doi:10.1016/J.RSER.2016.12.125

[6] P. N. Pakale, S. U. Patel, Performance Analysis Of Ic Engine Using Supercharger And Turbocharger-A Review, Int. J. Res. Eng. Technol., 4 (**2015**) 2, 17–22, doi:10.15623/ijret.2015.0402003

[7] A. Kusztelan, Y. F. Yao, D. R. Marchant, Y. Wang, A Review of Novel Turbocharger Concepts for Enhancements in Energy Efficiency, Int. J. Therm. Environ. Eng., 2 (**2010**) 2, 75–82, doi:10.5383/IJTEE.02.02.003

[8] B. P. Terani, K. S. Badarinarayan, Prakasha A M, Stability Analysis of Turbocharger Impeller: A Review, Int. Res. J. Eng. Technol., (**2015**)

[9] R. G. Kirk, E. J. Gunter, Stability analysis of a high-speed automotive turbocharger, Tribol. Trans., 50 (**2007**) 3, 427–434, doi:10.1080/10402000701476908

[10] R. G. Kirk et al., Experimental test results for vibration of a high speed diesel engine turbocharger, Tribol. Trans., 51 (**2008**) 4, 422–427, doi:10.1080/10402000801911853

[11] R. G. Kirk, A. A. Kornhauser, J. Sterling, A. Alsaeed, Turbocharger On-engine experimental vibration testing, JVC/Journal Vib. Control, 16 (**2010**) 3, 343–355, doi:10.1177/1077546309103564

[12] G. M. Ascanio, W. J. Wang, Diesel Engine Turbocharger Performance Monitoring Using Vibration Analysis, SAE Tech. Pap., 2007-September, (**2007**), doi:10.4271/2007-24-0082

[13] R. Holmes, M. J. Brennan, and B. Gottrand, Vibration of an automotive turbocharger – A case study, in IMechE Event Publications, (**2004**) 2, 445–455

[14] A. A. Alsaeed, Dynamic Stability Evaluation of an Automotive Turbocharger Rotor-Bearing System (2005)

[15] N. Sathishkumar, P. Premkumar, A. R. Bruce, K. Pravinkumar, P. L. Sudharsan, U. G. Scholar, Design and Analysis of an Impeller of a Turbocharger, Int. J. Res. Rev., 7 (**2020**) 4

[16] A. Singh, T. C. Gupta, Effect of rotating unbalance and engine excitations on the nonlinear dynamic response of turbocharger flexible rotor system supported on floating ring bearings, Arch. Appl. Mech., 90 (**2020**) 5, 1117–1134, doi:10.1007/s00419-020-01660-z

[17] N. M. Tammineni, R. R. Mutra, A review on recent advancements in an automotive turbocharger rotor system supported on the ball bearings, oil film and oil-free bearings, J. Brazilian Soc. Mech. Sci. Eng. 2023 459, 45 (**2023**) 9, 1–31, doi:10.1007/S40430-023-04383-8.

[18] D. R. Kumar, B. Shanmugasundaram, P. Mohanraj, Design and Analysis of Turbocharger Impeller in Diesel Engine, Int. J. Adv. Mech. Mech. Eng., 1 (**2017**) 1, 1–15

[19] P. Avitabile, Experimental modal analysis., Sound Vib., (**2001**) 1–11

[20] R. Gibson, Modal vibration response measurements for characterization of composite materials and structures, Compos. Sci. Technol., 60 (**2000**) 15, 2769–2780, doi:10.1016/S0266-3538(00)00092-0

[21] J. R. Banerjee, Frequency dependent mass and stiffness matrices of bar and beam elements and their equivalency with the dynamic stiffness matrix, Comput. Struct., 254 (**2021**), 106616, doi:10.1016/j.compstruc.2021.106616